

Late amagmatic extension along the central and eastern segments of the West Philippine Basin fossil spreading axis

Anne Deschamps^{a,*}, Kyoko Okino^b, Kantaro Fujioka^c

^a JAMSTEC, Deep Sea Research Department, 2-15 Natsushima-cho, Yokosuka 237-0061, Japan

^b Ocean Research Institute, University of Tokyo, 1-15-1 Minamidai, Nakano-ku, Tokyo 164, Japan

^c JAMSTEC, Frontier Research System for Extremophiles, 2-15 Natsushima-cho, Yokosuka 237-0061, Japan

Received 25 February 2002; received in revised form 2 July 2002; accepted 23 July 2002

Abstract

The spreading processes within the West Philippine Basin (WPB) remain partly unknown. This study presents an analysis of the tectono-magmatic processes that happened along its spreading axis during the conclusion of the last spreading phase at 33/30 Ma. We demonstrate that the late episode of N–S opening from an E–W-trending spreading system has been followed by a late tectonic event occurring in the central and eastern parts of the basin. This event was responsible for transtensional strain accommodated along the NW–SE faults cutting through the former E–W rift valley in the central part of the basin. In its eastern part, the same event occurred at a larger extent and led to the creation of a new NW–SE axis, obliquely cutting the older E–W spreading segments and their associated spreading fabrics. At this location, several tens of kilometers of slightly oblique amagmatic extension occurred following a $\sim 60^\circ$ direction. We propose that this late event is associated with the onset of E–W opening of the Parece-Vela Basin located along the eastern border of the WPB at 30 Ma. Extensive stresses within this basin were probably transmitted to the hot and easily deformable rift zone of the WPB. The newly-created NW–SE axis most likely propagated from east to west, being responsible for scissors opening within the WPB. NE–SW extension ceased when well-organized spreading started at 26 Ma in Parece-Vela Basin, accommodating entirely the global extensive stress pattern.

© 2002 Elsevier Science B.V. All rights reserved.

Keywords: West Philippine Basin; Philippine Sea Plate; spreading centers; seafloor spreading; segmentation; transform faults; discontinuities

1. Introduction

The West Philippine Basin (WPB) is a currently inactive marginal basin belonging to the Philip-

pine Sea Plate. The most recent model proposed for the spreading processes within the basin is from Hilde and Lee [1]. These authors analyzed magnetic anomalies and seafloor structures to propose a formation of the basin during two phases of spreading (Fig. 1). The first one probably occurred following a NE–SW direction between 58 and 45 Ma, and was followed by a second N–S episode along E–W-oriented spreading segments between 45 and 33 Ma, date of cessation

* Corresponding author. Tel.: +81-468-67-9339;
Fax: +81-468-67-9315.
E-mail address: deschamps@jamstec.go.jp (A. Deschamps).

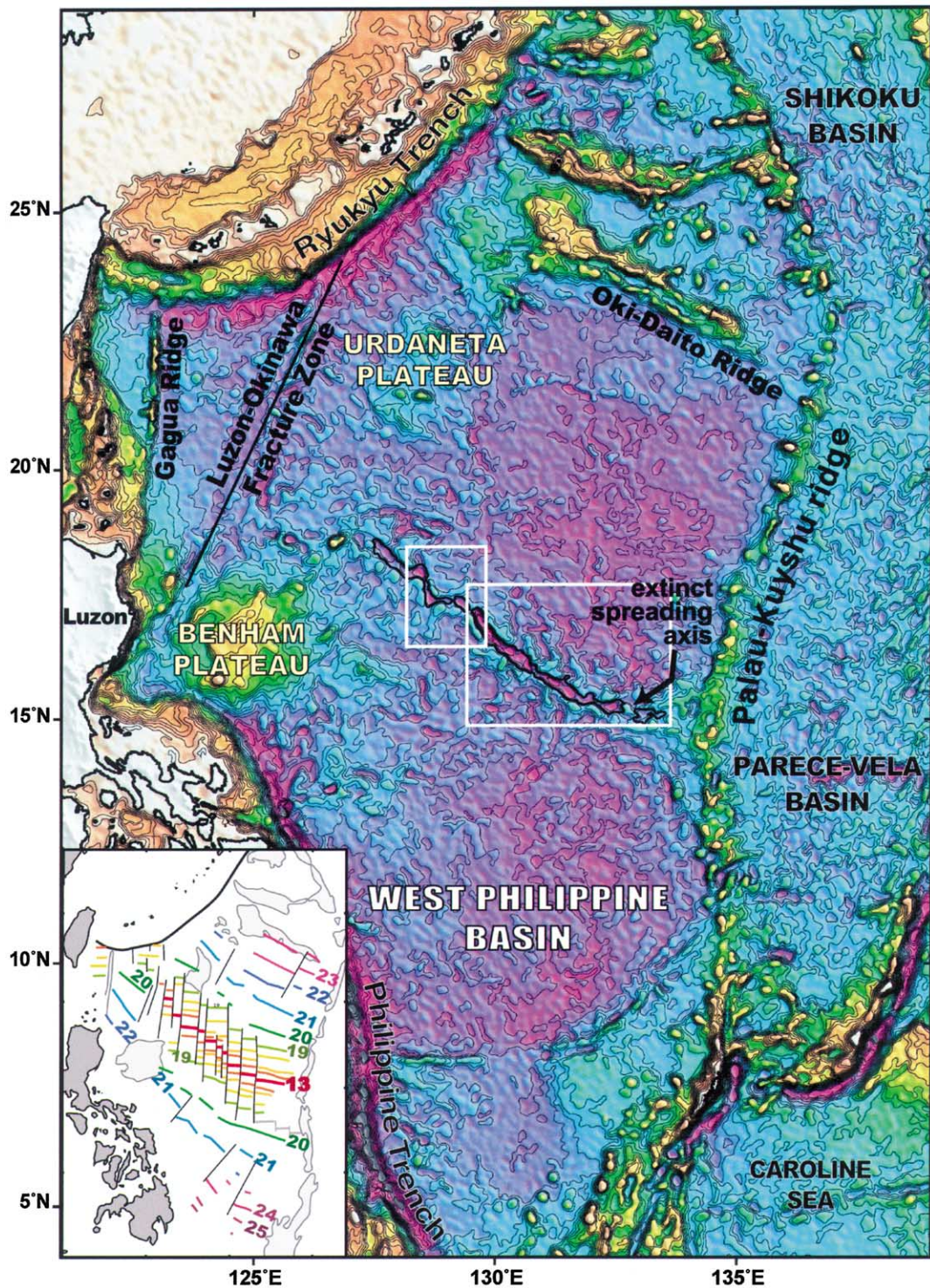


Fig. 1. Shaded contour view of the West Philippine Basin. Isocontour every 200 m. Major seafloor features of basin are labeled. White boxes indicate the locations of Figs. 2 and 3. Magnetic anomalies identified by Hilde and Lee [1] are shown.

of the spreading. Both episodes are believed to have occurred from a unique spreading axis that underwent a counter-clockwise reorientation and segmentation at 45 Ma. According to this model, the Benham and Urdaneta plateaus were formed by an excess of volcanism at the WPB spreading axis, due to the presence of a mantle plume in the western part of the basin during its opening. Concerning the global evolution of the Philippine Sea Plate, the most recent models are proposed by Hall [2] and Deschamps and Lallemand [3].

More recently, spreading processes within the WPB were revisited in the light of recent data collected in the basin [4–6] (Figs. 1–3). These studies allow to better define a new evolution model of the WPB. They reveal some discrepancies between the former spreading model [1] and the seafloor and rift valley morphology:

1. The global NW–SE orientation of the rift valley and bounding scarps is hardly explained by the last N–S spreading phase that is supposed to have occurred from an E–W spreading axis.
2. Magnetic anomalies identification suggests that spreading ended at 33 Ma [1] (Fig. 1) and 33/30 Ma [3]. Ages obtained from basalt samples collected directly within the rift valley range from 26.1 to 28.1 Ma (Ar/Ar method) [5,6] (Fig. 3), which is much younger than the age of the end of spreading deduced from magnetic anomalies.
3. The bottom of the rift valley is as deep as 7900 m, that is much deeper than other well-known active or inactive spreading centers.
4. Bathymetric data show that most of the N–S non-transform discontinuities that stand on both sides of the rift valley do not face each other, but are rather dextrally offset. We suspect that tectonic and magmatic activity along the rift valley did not simply resume with the end of the N–S spreading phase, but rather after another event that occurred in this region.

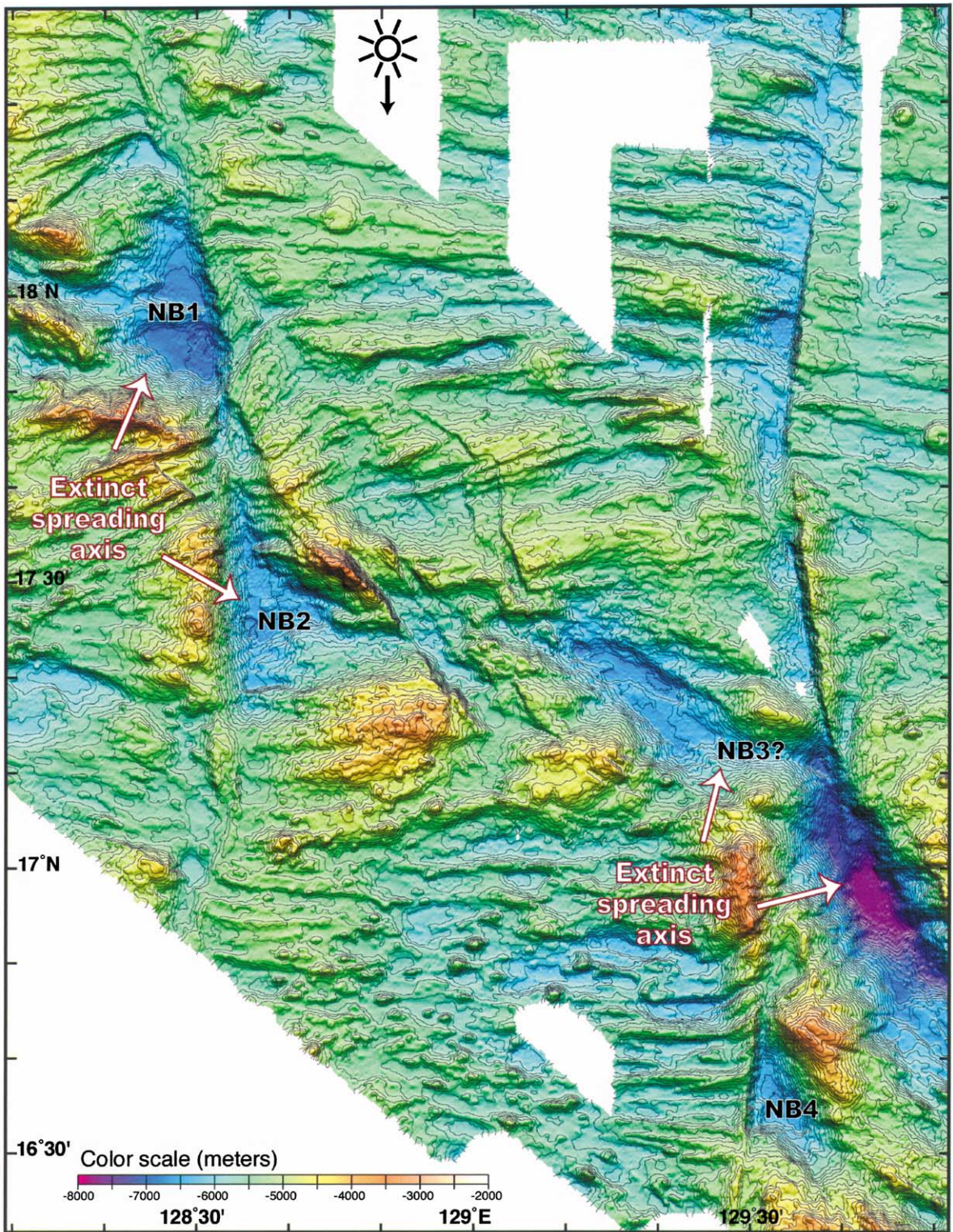
Such observations justify to revisit the spreading history of the WPB, specifically the period

before the end of spreading. In this paper we present detailed seafloor structures in the vicinity of the spreading axis. Their study allows us to analyze the tectonic and magmatic processes that occurred during the last 100 km of seafloor generation in the basin (Fig. 1). Our study focuses mainly on the central and eastern parts of the spreading axis, because these areas were not under the influence of the mantle plume that was active in the western WPB during spreading [3,7]. They are therefore well suited for a study of the last events that took place at the WPB spreading axis. Our study gives evidence of a late and short stage of ~NE–SW amagmatic extension that followed the last N–S stage of spreading. This event explains the abnormal great depth of the rift valley, its atypical orientation as well as other characteristics that we mentioned above.

2. Seafloor morphology near the spreading axis

Recent geophysical data were acquired in the vicinity of the WPB fossil spreading axis during Japanese and French cruises [4,5,8,9]. Between 1998 and 2000, *R/V Kairei* and *R/V Yokosuka* conducted geological and geophysical surveys of the rift valley during the cruises KR9801, KR9812, KR9910 and YK0001. Swath bathymetry using Sea Beam 2112, magnetic and gravity data were collected as well as dredges and piston core samples [5,9,10]. The primary track lines were NW–SE-oriented, parallel to the general trend of the spreading axis. These data were merged with swath bathymetry data from the *R/V L'Atalante*, acquired in 1996 and 1997 during the KAONOUM and DAVAPUS transects. During these transects, a SIMRAD EM12-Dual multibeam swath-mapping system was used to collect bathymetric and backscatter data across a maximum 20 km wide swath of the seafloor in a single pass (with 151 beams) [4,8,11]. Magnetic and gravity data are discussed by Okino et al. [12]. In this paper, we present bathymetric data over

Fig. 2 (Figure overleaf). Shaded bathymetric relief of central West Philippine Basin. Isocontour every 100 m. Nodal basins mentioned in text are called NB1, NB2, NB3, and NB4. Corresponding structural map with terminology is shown in Fig. 4.



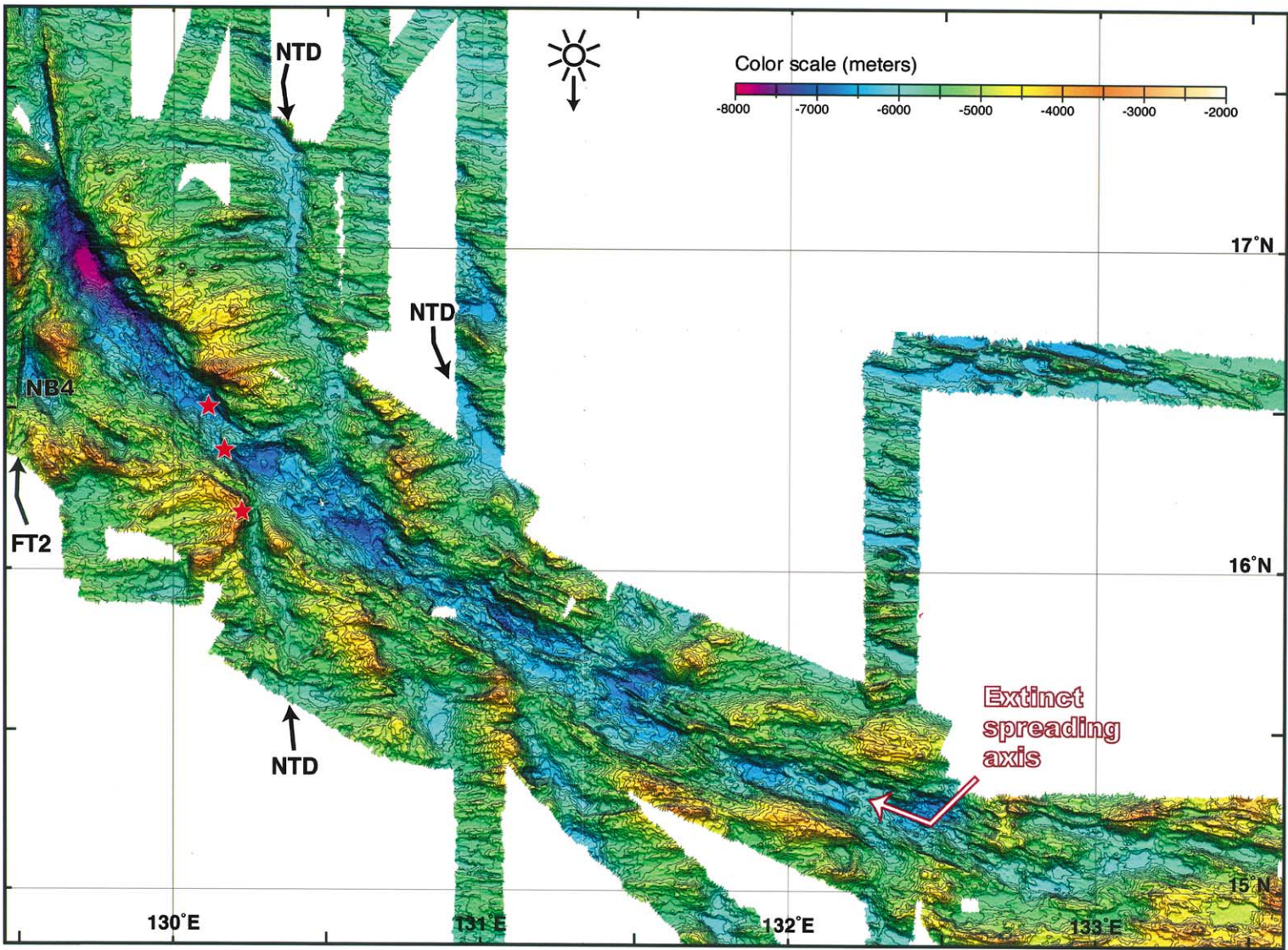


Fig. 3. Shaded contour bathymetric map of eastern West Philippine Basin. Isocontour every 100 m. FT2: transform fault 2; NTD: non-transform discontinuity; NB4: possible remnant nodal basin. Corresponding structural map with terminology is shown in Fig. 5. Stars represent dive or dredge sites where igneous rocks were recovered for dating.

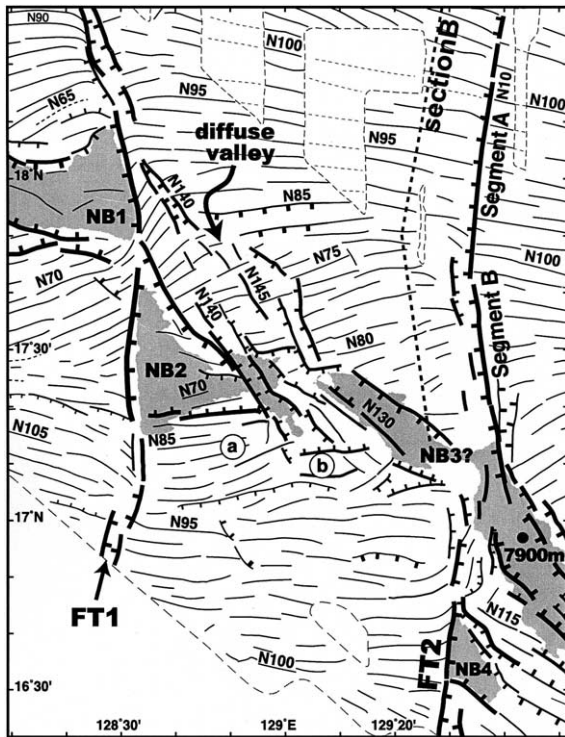


Fig. 4. Structural map of the central basin. FT1: transform fault 1; FT2: transform fault 2; NB1, NB2, NB3: nodal basins defined by the deepening of the rift valley when approaching the transform fault; NB4: possible remnant nodal basin. Hachured lines indicate main fault scarps. Dashed dark heavy line corresponds to the location of the bathymetric profile B shown in Fig. 6.

a 100 km wide strip including the rift valley (Figs. 2 and 3).

2.1. Trend and height of abyssal hills

In the central and eastern parts of the basin, $\sim 95/100^\circ$ -trending abyssal hills are well organized at a distance of 100 km from the fossil rift valley. They gradually rotate counter-clockwise when approaching the rift valley, and finally strike $\sim 80/70^\circ$ close to it (Figs. 2–5) [5]. They are continuous over distances often exceeding 60 km. Far from the spreading axis, their height varies from 100 to 400 m, and their spacing ranges from 3 to 8 km (Fig. 6A). Their relief and spacing increase significantly when approach-

ing the spreading axis. Close to it, abyssal hills are 500–1200 m high, and the wavelength of crests is 7–11 km (Fig. 6A, B).

2.2. Morphology of first-order discontinuities

In the central part of the basin, first-order segmentation of the fossil spreading axis is marked by the occurrence of two 100-km-spaced, N–S-trending transform faults (TF) (Figs. 2 and 4). The westernmost one (FT1) is continuous over at least 160 km. The rift valley is dextrally offset along the FT1 by 80 ± 20 km (Fig. 4). Fujioka et al. [5] notice that (1) the floor of the rift valley deepens and widens when approaching FT1, (2) small topographic troughs (nodal basins NB1 and NB2) occur at the ridge–transform intersection (RTI) [13,14], and (3) large topographic highs, called inside corner highs, are observed on the transform side of the rift valley. They deduced that the morphology of this spreading axis is characteristic of a slow spreading axis as described by Blackman and Forsyth [15] and Bonatti et al. [16]. The easternmost TF (FT2) is expressed over at least 220 km. The rift valley is apparently only slightly offset by this fault, but the small triangular-shaped basin that is observed around $129^\circ 30' E / 16^\circ 35' N$ (NB4) probably represents a former nodal basin. In this case, the initial dextral offset of the axial rift valley is 70 ± 30 km.

2.2.1. FT2 morphology

The fault FT2 is well marked in morphology (Figs. 2 and 4). Its northern segment displays a general N–S trend. It consists of a west-facing escarpment that can be divided into two segments (A and B) based on orientation and morphological criteria (Fig. 4). The seafloor roughness varies on both sides of the northern part of FT2. At $18^\circ N$, for example, the seafloor is relatively smooth east of the fault, with abyssal hills having a 40–200 m relief and an average 4 km spacing (Fig. 6A), whereas west of FT2 the sea bottom looks rougher with 400–800-m-high abyssal hills (up to 1 km) that are 9 km spaced in average (Fig. 6B).

Segment A of FT2 is linear and trends $\sim 10^\circ$, remaining strictly perpendicular to the surround-

rate was intermediate with a half-rate of 4 cm/yr, which means that the difference in age on both sides of the FT2 should be only ~ 2 Ma considering a dextral offset of 70 km. This confirms that the scarp observed along the northern part of FT2 is not due to the age difference across the fault because it is too small to induce significant differences in the thermal evolution of both sides of the FZ.

Segment B of FT2 is linear and trends $\sim 170^\circ$ (Figs. 2 and 4). As segment A, it faces west but is much higher (up to ~ 1300 m). The presence of a discrete ~ 700 -m-high transverse ridge forming the eastern wall of the TF valley suggests a localized deformation resulting from changes in the spreading system. From the study of the Mid-Atlantic Ridge between 21 and 24°N , Pockalny et al. (1996) [19] demonstrate that a clockwise change in spreading direction near a large-offset, right-stepping TF is able to account for the presence of transverse ridges. These ridges result from minor extension (< 5 km) along low-angle ($< 45^\circ$) normal faults. Conversely, when a spreading axis undergoes a counter-clockwise reorientation, an active right-stepping TF experiences a compressive deformation during a short time before a new transform fault is created perpendicular to the newly-oriented spreading segment. This phenomenon is generally the cause for the uplift of a compressive transverse ridge similar to the one that we observe along segment B (e.g. [20–24]). The spreading fabric that is located north of this ridge trends $\sim 100^\circ$ (see above) whereas it trends

$\sim 90/80^\circ$ more to the south, suggesting such a progressive counter-clockwise reorientation of the spreading axis during spreading (Figs. 2 and 4).

The segment of FT2 that is located south of the spreading axis consists in a $\sim 5^\circ$ east-facing escarpment. The height of this scarp culminates ~ 1300 m above the relic of the nodal basin NB4 (at $129^\circ 30'\text{E}/16^\circ 35'\text{N}$). West of the scarp, the spreading fabric trends $\sim 100^\circ$ and progressively turns to a $\sim 80^\circ$ orientation when approaching the rift valley, suggesting a counter-clockwise rotation of the spreading axis, which is consistent with former observations of the northern segment of FT2.

When approaching FT2, abyssal hills suddenly turn southwards to the south of $16^\circ 30'\text{N}$, but northwards to the north of this latitude. Such a curvature of spreading fabric close to a TF is common and is due to a change of the stress pattern near the fault (e.g. [13,25,26,27]). However, if the southward curvature of hills is consistent with a shear couple due to a retarded plate motion along the transform [28], their northward curvature north of $16^\circ 30'\text{N}$ is unusual. Such inconsistencies in hill curvatures are observed near Bullard and Clipperton TFs and are the result of a counter-clockwise rotation of a right-stepping spreading axis that causes the formation of a shear couple leading to the rotation of abyssal hills [28,29]. Along the southern segment of FT2, the change in the curvature of abyssal hills coincides with the reorientation of the surrounding spreading fabric and confirms a counter-clock-

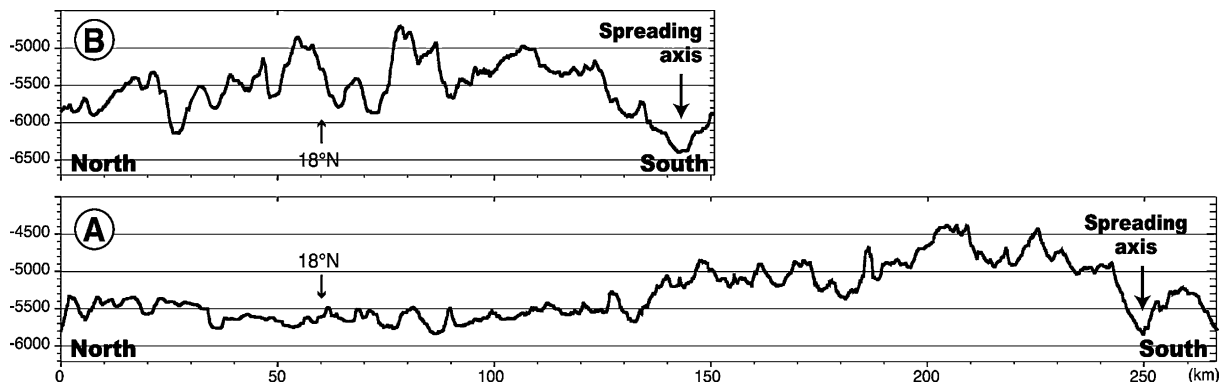


Fig. 6. Bathymetric profiles perpendicular to the spreading fabric located north of the rift valley. Locations of profiles in Figs. 4 and 5.

wise rotation of the spreading axis about 50 km before the end of spreading. The small and narrow, 500-m-high ridge forming the western wall of the transform valley south of 16°50'N is probably due to a localized compression resulting from the rotation of the spreading system. North of this latitude, the height and the morphology of this ridge drastically change, which rather suggests a volcanic origin.

2.2.2. FT1 morphology

The fault FT1 displays a global N–S orientation. Northward, it trends $\sim 10^\circ\text{W}$ but N–S and $\sim 10^\circ\text{E}$ toward the south (Figs. 2 and 4). The westward curvature of the northern segment of FT1 is due to its interaction with a microplate that developed immediately to the west. We ignore this area located west of 128°10'N since its development was influenced by the presence of a mantle plume [3,7]. The segment of FT1 that is located south of the spreading axis is characterized by an east-facing escarpment north of 17°20'N. South of this latitude, the morphology of the fault zone is subtler. At this location, the fault trends $\sim 10^\circ$ at a right angle with the spreading fabric, suggesting that spreading occurred from a $\sim 100^\circ$ -trending spreading segment. Northward, the fault trends more N–S and the height of its western wall reaches ~ 2 km above the nodal basin NB2. The reduced depth of the seafloor at this location can be due to an intense magmatism combined with a compressive deformation related to a reorientation of the spreading axis. The spreading system indeed most likely underwent a counter-clockwise reorientation from a $\sim 100^\circ$ to a $\sim 80^\circ$ trend during the end of spreading, as shown by the orientation of abyssal hills and by our study of the FT2 and its surroundings (Section 2.2.1). This reorientation of the spreading system is probably responsible for transpression along right-stepping transforms that caused seafloor fabric on the east side of FT1 to curve towards the ridge axis [30,31].

2.2.3. Significance of transform faults FT1 and FT2

The similarity between morphologies of the faults FT1 and FT2 suggests that both result

from the same spreading history, i.e. a former $\sim 100^\circ$ right-stepping spreading axis that underwent a counter-clockwise rotation of $\sim 20^\circ$ about 3 Ma before the end of spreading if considering a half-spreading rate of ~ 2 cm/yr during the last spreading phase [1].

2.3. Morphology of the second-order discontinuities

There is no significant segmentation of the rift axis east of FT2 (Fig. 3). However, on both sides of the rift axis, several sinuous valleys interrupt the seafloor fabric every 50 ± 20 km. These valleys are 10–30 km wide and at least 110 km long. They globally trend N–S (Figs. 3 and 5). Their orientation slightly changes together with the spreading fabrics always remaining at a right angle with them. Their morphology is similar to the non-transform discontinuities (NTDs) observed along the Mid-Atlantic Ridge [32,33]. The offset of the spreading axis along them varies from 0 to 30 km. Spreading segments limited by NTDs are 50 ± 30 km in length. According to the hypothesis that each spreading segment is the locus of focused mantle upwelling (e.g. [18,34,35]), their length is dependent on the quantity of injected magmas and then is likely to vary as a function of the magmatic budget [36]. Spreading segments that are bordered by NTDs may thus have their length varying with time [33,37]. This is what we observe near the WPB spreading axis.

It should be pointed out that NTDs on both sides of the rift valley do not exactly face each other, but are offset right-laterally by about 30–40 km. This cannot be explained simply by a basic N–S spreading phase. Section 4.2 will be devoted to the analysis of NTDs' arrangement.

2.4. Evolution of the spreading processes

The gradual rotation of abyssal hills in conjunction with the reorientation of TFs and NTDs that remain perpendicular to them suggests a rotation of the spreading axis during spreading, with respect to the lithosphere that has been previously formed. Hundred kilometers away from the present rift axis, the spreading direction was

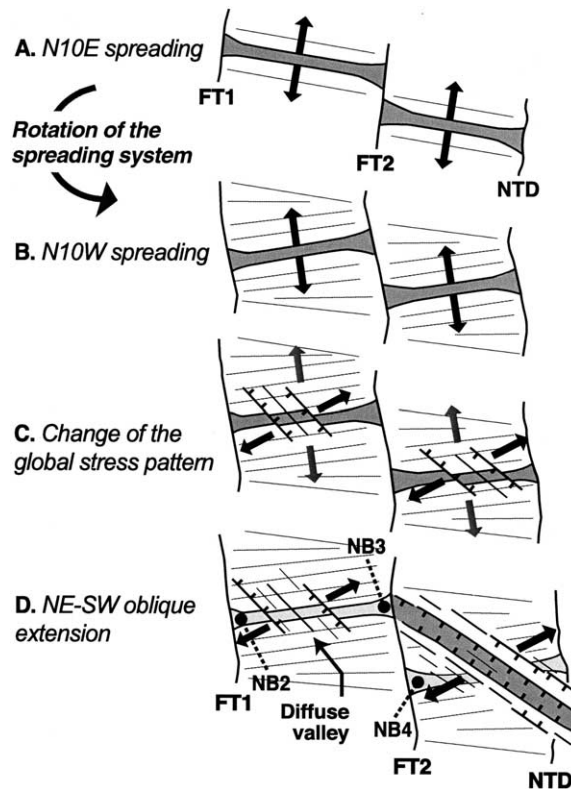


Fig. 7. Sketch showing the evolution of the West Philippine Basin axis during its last 100 km of activity. FT1: transform fault 1; FT2: transform fault 2; NB: nodal basins defined by the deepening of the rift valley when approaching the transform fault. For explanations see Section 4.1.

$\sim 10^\circ\text{E}$ and gradually changed to $\sim 10^\circ\text{W}$ close to the axis, i.e. at the end of spreading. This conclusion rests on the hypothesis that the spreading direction is perpendicular to the trend of seafloor fabric. This is reasonable since abyssal hills always remain perpendicular (within $\sim 5^\circ$) to the spreading direction even in the case of oblique rifting as observed along the Reykjanes and Mohns ridges (Norwegian Sea) [38,39], and also along the Gulf of Aden rift [40].

The morphology and spacing of abyssal hills indicate that spreading occurred at an intermediate to slow rate. Their increasing height and spacing toward the spreading axis reveal a slowing down of the spreading rate synchronous with a decreasing magma supply. These conclusions are based on the comparison of the morphologic characteristics of abyssal hills in the West Philippine Basin with other similar structures observed

along other well-known spreading axes. For example, abyssal hills formed along the slow Mid-Atlantic Ridge are 400 to more than 1000 m high, with a spacing that varies from 2.5 to 9 km, depending on the location of the bathymetric profile in the middle or extremity of a spreading segment [41]. Another study of the intermediate spreading of Ecuador Rift reveals 50–150-m-high and 1.5-km-spaced abyssal hills [42]. The rate of spreading deduced from the morphology of abyssal hills correlates with values proposed by Hilde and Lee for the WPB [1].

The presence of NTDs east of FT2 is consistent with a slow rate of spreading and a reduced magma supply, according to the hypothesis of Sloan and Patriat [37] and Detrick et al. [36]. It also indicates that spreading segments were only slightly offset (< 30 km) during this last episode of spreading.

3. Morphology of the rift valley

3.1. A deep valley cutting across the spreading fabric in the eastern basin

East of 129°30'E, the spreading axis is expressed by a continuous deep valley that trends $\sim 140^\circ$, but gradually turns to a $\sim 110^\circ$ orientation near the Palau-Kyushu Ridge (PKR) (Figs. 3 and 5) [12]. The valley is 20–30 km wide and ~ 6500 m deep on average. It locally reaches 7900 m (129°45'E/16°55'N) (Fig. 5). When approaching the PKR, it shallows at ~ 5800 m. The valley is bordered by scarps related to normal faults active during extensional processes at the rift axis. Their height increases from east to west as the valley deepens: the vertical offset is often ~ 500 m in the vicinity of the PKR (at 133°E) and frequently more than 2500 m near 129°340'E (Fig. 3). West of 132°30'E, scarps cut the off-axis spreading fabric straight (see a, b, c in Fig. 5). The width of the area where scarps and abyssal hills parallel the rift valley is very limited, and rarely exceeds ~ 15 km on each side.

3.2. NW–SE faults interrupt the rift valley in the central basin

In the central part of the basin, the general trend of the rift valley is $\sim 100^\circ$ (Figs. 2 and 4). Its depth is 5600 m on average. It reaches 6600 m at the bottom of the nodal basins close to FT1 and FT2. Unlike in the eastern part of the basin, the scarps bounding the rift valley parallel the $\sim 80^\circ$ -trending off-axis spreading fabric and do not cut through it.

Between FT1 and FT2, the rift valley and off-axis spreading fabric are partially interrupted by $\sim 140^\circ$ -trending linear fault scarps (Figs. 2 and 4). These faults can be followed over distances of 10–50 km. The vertical offset along the scarps reaches ~ 1200 m, suggesting that normal movement has occurred along them. A small amount (~ 20 km in total) of dextral strike-slip faulting most likely occurred along these fault planes since they only slightly offset the rift valley right-laterally. These scarps delineate areas with contrasting

reliefs (see a, b in Fig. 4) similar to inside corner highs which are commonly observed on the transform sides of rift valleys [5]. This suggests that the activity of these faults started when spreading was still occurring from the $\sim 80^\circ$ -oriented spreading axis.

Finally, the movement that occurred along $\sim 140^\circ$ fault planes during the last 50 km of $\sim 10^\circ$ W-directed opening resulted in a gradual dextral offset of the former $\sim 80^\circ$ rift valley and in the creation of a diffuse $\sim 140^\circ$ -oriented valley in the central part of the WPB (Fig. 4).

4. Discussion: Modalities of spreading during the last spreading phase

4.1. Significance of the NW–SE orientation of faults and rift valley

In the eastern part of the basin, the rift valley trends highly obliquely ($\sim 140^\circ$) to the off-axis spreading fabric ($\sim 80^\circ$) (Section 3.1). In our interpretation, the present-day structure results of a brutal jump and a reorientation of the spreading axis (Fig. 7). There is only indirect evidence for the existence of the former $\sim 80^\circ$ spreading segments, as e.g. the $\sim 80^\circ$ orientation of off-axis abyssal hills, the $\sim 10^\circ$ W trend of the NTDs, and the remnant nodal basin NB4. We rule out the hypothesis of oblique rifting (Fig. 8) to explain the obliquity between the rift valley and the former spreading fabric, based on several reasons: (1) abyssal hills are linear and continuous over important distances, but should be less long (< 20 km) and sigmoidal, en echelon or interconnected in case of oblique rifting (Section 2.1) [38], (2) the $\sim 140^\circ$ rift valley abruptly cuts across the $\sim 80^\circ$ spreading fabric, and (3) in some areas (near 130°E), spreading should have occurred with $\sim 50^\circ$ of obliquity during the formation of at least 80 km of seafloor, in case of oblique rifting (Fig. 8). Examples of such a high obliquity during such a long duration of opening have never been described. This type of system, if it exists, is supposed to be unstable and to evolve rapidly toward a more stable configuration, i.e. the formation of a new spreading axis perpendic-

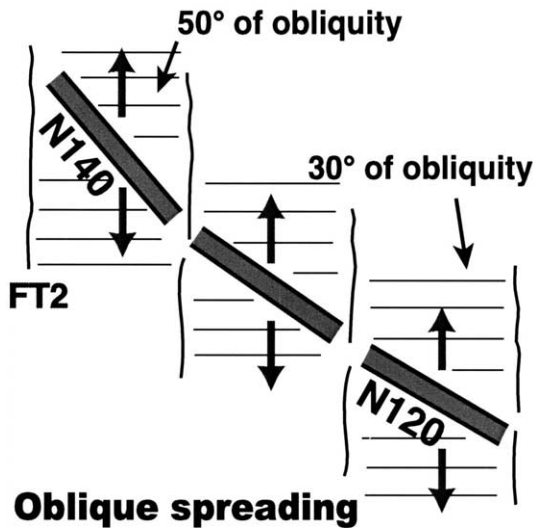


Fig. 8. Sketch quantifying the obliquity of spreading in case of oblique spreading. For explanations see Section 4.1.

ular to the opening direction [39], which is not what we observe.

We propose that a last phase of \sim NE–SW extension occurred in the eastern part of the basin from a newly-created NW–SE rift valley replacing the former E–W one. The important depth of the new valley and the great height of fault scarps that bound it indicate that tectonic processes have predominated over magmatic processes during this last event. The reduced width of the seafloor strip displaying structures parallel to the new axis (Section 3.1) favors a short-lived event. In the central part of the basin (between FT1 and FT2), the same processes occurred but to a lesser extent. In this area, the \sim 140° faults that cut across the \sim 80° former rift are most likely related to tectonic events that led to the creation of the new NW–SE rift valley observed further to the east. Movements along the \sim 140° fault planes did not result here in the genesis of a well-marked and deep valley (Fig. 7). It seems therefore that the tectonic effects of the last NE–SW extension episode varied in space: the activity of the \sim 140° faults resulted in the creation of a new NW–SE rift valley followed by \sim NE–SW extension in the eastern part of the basin. Further to the west, bathymetric features do not evidence such a

strong extension episode. This may reveal scissors opening with the new NW–SE axis viewed as rift propagating from east to west.

In the easternmost part of the basin, the newly-created rift valley displays a \sim 110° trend. East of 132°30'E, its associated seafloor structures do not cross cut the off-axis abyssal hills (Section 3.1). A late stage of \sim NE–SW extension probably also occurred in this area as shown by the obliquity between the rift valley and the off-axis spreading fabric. However, we suggest that in the central part of the basin, the former spreading axis was abruptly cut across by the new NW–SE rift valley whereas, in its easternmost part, the weak and hot zone that characterized the former spreading axis was partly re-used to accommodate the \sim NE–SW opening obliquely.

4.2. Characteristics of the displacement along the newly-created NW–SE rift valley and faults

We have shown how the NW–SE faults observed in the vicinity of the spreading axis underwent normal movements leading to the creation of a more or less developed NW–SE rift valley, depending on the location (Section 4.1). In the central part of the basin, \sim 20 km of right-lateral displacements possibly occurred along the NW–SE faults (Section 3.2) (Fig. 2). This suggests that the last stage of extension occurred slightly obliquely to these fault planes. In the eastern part of the basin, NTDs on both sides of the rift valley seem to be dextrally offset (Section 2.4). We thus infer that extension that occurred along the newly-formed NW–SE rift valley in this part of the basin was also slightly oblique. We ‘closed’ the basin perpendicularly to the NW–SE structures associated with the last \sim NE–SW extensional event, such that we can observe the former location of NTDs before the new NW–SE axis was created (Fig. 9). We selected landmarks such as NTD valleys or bathymetric highs that stand on both of its sides and whose morphology suggests they could have a common origin. Finally, when the basin is closed following a direction at a right angle to the NW–SE faults associated with the new valley, the respective locations of landmarks indicate that they remain dextrally

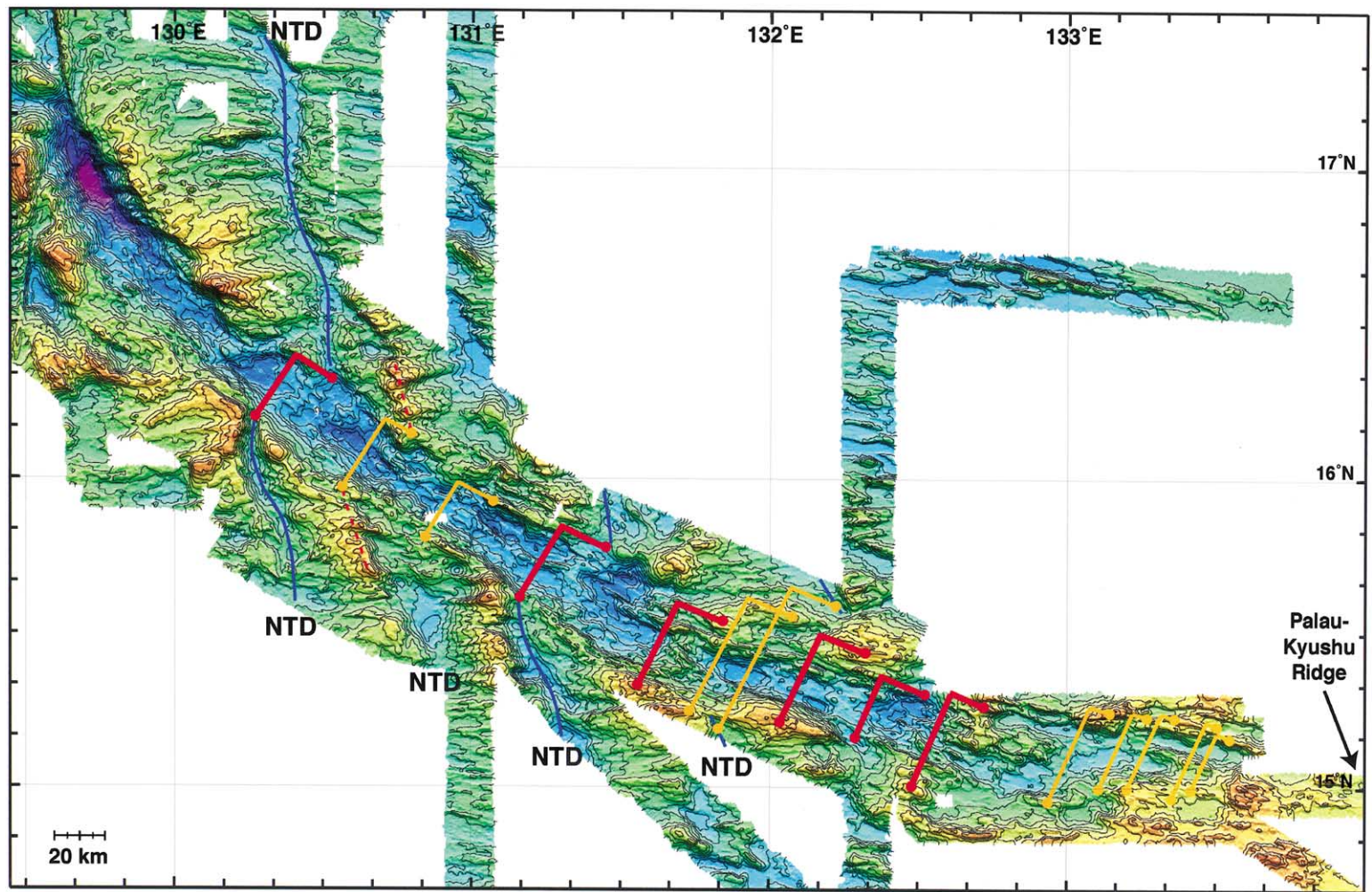


Fig. 9. Quantification of the right-lateral offset of the seafloor on both sides of the newly-formed rift valley. NTD: non-transform discontinuity. Lines indicate the path between two similar features located on both sides of the valley. Red lines indicate paths between reliable markers. Yellow lines show paths connecting less trustworthy topographic reliefs. For details see [Section 4.2](#).

offset by a distance of 15–18 km (Fig. 9). The extension that occurred from the new NW–SE rift valley and along its associated fault planes was thus slightly oblique following a $\sim 60^\circ$ direction (Fig. 7).

4.3. *When did the last NE–SW extension episode take place?*

The $\sim 10^\circ\text{W}$ spreading phase had not finished yet when activity began along the NW–SE faults in the central part of the WPB (Section 4.2). We suggest that the $\sim 60^\circ$ extension event began during the end of the spreading in the WPB at $\sim 33/30$ Ma [1,3,7]. We cannot estimate its exact duration, but 28–26 Ma ages determined on basalts from the rift walls [5] could be related to magma emplacement during this event. The $\sim 60^\circ$ -directed episode of the opening therefore most likely lasted for several millions of years from 33/30 Ma to 26 Ma.

4.4. *Possible cause of the last event along the WPB spreading axis*

The occurrence of a $\sim \text{NE–SW}$ episode of extension shortly after the $\sim 10^\circ\text{W}$ phase of spreading reveals an important and abrupt change in the stress pattern within the WPB and its margins. Before 33 Ma, the WPB was subjected to extensive stresses transmitted from its northeastern boundary because of the westward subduction of the old Pacific Plate along the Palau-Kyushu Ridge [2,3,7]. The 33/32 Ma period corresponds to the incipient collision between the northern part of the Philippine Arc with rifted fragments of the Eurasian continental margin [43]. This collision led to a compressive episode along the western margin of the basin, to the uplift of the Gagua Ridge (Fig. 1) and to a short subduction episode of the WPB beneath East Luzon [44]. This last subduction episode resumed at ~ 30 Ma, due to incipient subduction along the Manila Trench [43]. A change in the relative motion of the Pacific Plate is also inferred at ~ 33 Ma, based on a study of fracture zones, magnetic anomalies and hotspot chains [45,46]. This change probably initiated rifting in the Japan Sea and in the Parece-

Vela and Shikoku basins since the Late Oligocene [47,48].

We suspect that the end of the $\sim 10^\circ\text{W}$ phase of spreading as well as the last $\sim \text{NE–SW}$ extensive event are related to both Early Oligocene tectonic events mentioned above. Since ~ 33 Ma, the western boundary of the WPB has constituted a locked boundary while extensive constraints related to incipient E–W rifting in the Parece-Vela Basin were probably transmitted since ~ 30 Ma to the former WPB spreading axis which constituted a hot zone of weakness. A late stage of oblique opening occurred and probably ceased when organized spreading started at ~ 26 Ma in the Parece-Vela Basin [48], that means when its opening began to fully accommodate the global extensive stresses.

4.5. *Possible causes of the spatial variation of the last NE–SW extension event*

The last phase of $\sim \text{NE–SW}$ extension led to the creation of a new rift valley followed by extensional deformation in the eastern part of the WPB whereas, in its central between FT1 and FT2, it only led to the formation of a less well-defined valley. We propose two explanations for such a variation in space of this last event:

1. In the western part of the WPB, the presence of an active hotspot during spreading most likely caused the lithosphere to be hotter and characterized by a shallow depth of the brittle–ductile transition with respect to the eastern part of the basin. Then, in the western part of the basin, extensive stresses related to the $\sim \text{NE–SW}$ event were accommodated in a diffuse pattern within an easily deformable lithosphere. This is confirmed by the existence of syn-volcanic pull-apart structures further to the west between $127^\circ 30'\text{E}$ and 128°E [4] that show that transtension also occurred in this area and was accommodated by almost ductile deformation.
2. We showed in Section 4.4 that the late $\sim \text{NE–SW}$ extension episode probably originated from the eastern side of the basin. This led possibly to scissors opening with the new

NW–SE rift that propagates from east to west. Thus, it could be explained why associated structures are better developed in the eastern part of the basin than in its western part.

5. Conclusion

New data collected in the vicinity of the West Philippine Basin spreading axis make it possible to define more accurately the anatomy and functioning of the fossil spreading axis during its last million years of activity. They reveal that magmatic and volcanic activity within the basin did not resume simply during a last stage of N–S spreading as previously inferred, but after a last event of slightly oblique amagmatic extension along a newly-created NW–SE rift valley.

Several million years before the end of the spreading, opening occurred along a $\sim 10^\circ$ direction from a right-stepping $\sim 100^\circ$ -trending axis at an intermediate spreading rate (Fig. 7). About 3 Ma before the cessation of spreading at $\sim 33/30$ Ma, the spreading system underwent a counter-clockwise rotation with respect to the previously formed lithosphere. The orientation of the spreading axis segments became E–W and then $\sim 80^\circ$. This rotation of the spreading system has been registered in the morphology of the transform faults and surrounding seafloor reliefs. The rate of spreading synchronously diminished significantly. The height and spacing of abyssal hills increased. Non-transform discontinuities developed in the eastern part of the basin.

Shortly before the end of spreading, a transtensional movement occurred along NW–SE-oriented faults cutting across the $\sim 80^\circ$ segments of the former spreading axis. In the central part of the basin, activity of these faults led to the creation of a diffuse NW–SE valley. In the eastern part of the basin, a well-expressed valley bordered by up to 2.5-km-high escarpments was created and an episode of \sim NE–SW extension occurred slightly obliquely to the NW–SE faults. This episode was brief, if compared to the long Early Eocene to Early Oligocene spreading history of the WPB. It was also characterized by a low supply in magma. The transtensional deformation

most likely contributed to the deepening of the deformation zone, explaining the great depth of the rift valley. The westward propagation of the new rift valley is responsible for scissors opening. The resulting deformation is thus subtler in the western part of the basin, even more so since extensive stresses were accommodated in this area by more ductile deformation due to the higher thermicity of the lithosphere.

The late \sim NE–SW extension event occurred sometime between 33/30 and 26 Ma. It is most likely related to a major change in the regional tectonic setting of its boundaries, i.e. the locking of the western boundary of the WPB whereas its eastern boundary was subjected to extensive stresses related to incipient E–W rifting in the Parece-Vela Basin since ~ 30 Ma. The deformation probably ceased due to the onset of well-organized spreading at ~ 26 Ma in this last basin.

Acknowledgements

We thank the crew and scientists onboard the *R/V L'Atalante* and *Yokosuka* for their efficient work during the Kaonoum survey and STEP IV cruise. Thanks to P. Gente, T. Fujiwara, Y. Lagabrielle and A. Nicolas for valuable discussions. I wish to thank Robert Pockalny and an anonymous reviewer for their constructive criticism and helpful comments. Bettina and Jeff Schuffert are warmly acknowledged for English improvement of the paper. G.M.T. 3.3 from Wessel and Smith was used to map data. [AC]

References

- [1] T.W. Hilde, C.S. Lee, Origin and evolution of the West Philippine Basin: A new interpretation, *Tectonophysics* 102 (1984) 85–104.
- [2] R. Hall, Cenozoic geological and plate tectonic evolution of SE Asia and the SW Pacific: computer-based reconstructions and animations, *J. Asian Earth Sci.* 20 (2002) 353–431.
- [3] A. Deschamps, S. Lallemand, The West Philippine Basin, an Eocene to Early Oligocene back-arc basin opened between two opposed subduction zones, *J. Geophys. Res.*, submitted.
- [4] A. Deschamps, S.E. Lallemand, S. Dominguez, The last

- spreading episode of the West Philippine Basin revisited, *Geophys. Res. Lett.* 26 (1999) 2073–2076.
- [5] K. Fujioka, K. Okino, T. Kanamatsu, Y. Ohara, O. Ishisuka, S. Haraguchi, T. Ishii, Enigmatic extinct spreading center in the West Philippine backarc basin unveiled, *Geology* 27 (1999) 1135–1138.
- [6] K. Okino, Y. Ohara, S. Kasuga, Y. Kato, The Philippine Sea: a new survey results reveal the structure and history of the marginal basins, *Geophys. Res. Lett.* 26 (1999) 2287–2290.
- [7] A. Deschamps, Contribution à l'étude du Bassin Ouest Philippin: nouvelles données sur la bordure Ouest et la dorsale fossile - Contribution to the study of the West Philippine Basin: new data on the western boundary and the fossil spreading center, Ph.D. thesis, University of Montpellier 2, Montpellier, 2001, 247 pp.
- [8] S.E. Lallemand, Liu C.-S. and the ACT scientific crew, Swath bathymetry reveals active arc-continent collision near Taiwan, *EOS Trans. AGU* 78 (17) (1997) 173–175.
- [9] K. Fujioka, T. Kanamatsu, Y. Ohara, H. Fujimoto, K. Okino, C. Tamura, S.E. Lallemand, A. Deschamps-Boldrini, J.A. Barretto, N. Togashi, H. Yamanobe, A. So, Parece Vela Rift and Central Basin Fault revisited; STEPS-IV (structure, tectonics and evolution of the Philippine Sea), cruise summary report, *InterRidge News* 9 (2001) 18–22.
- [10] T. Yamazaki, K. Okino, Y. Hasegawa, H. Saitake, M. Ito, Geophysical mapping of Mariana Trough and West Philippine Basin: a preliminary report of Kairei KR9812 cruise, *JAMSTEC J. Deep Sea Res.* 15 (II) (1999) 63–72.
- [11] S.E. Lallemand, M. Popoff, J.-P. Cadet, B. Deffontaines, A.-G. Bader, M. Pubellier, C. Rangin, Genetic relations between the central and southern Philippine Trench and the Philippine Trench, *J. Geophys. Res.* 103 (B1) (1998) 933–950.
- [12] K. Okino, K. Fujioka, The central basin spreading center: variations in spreading style and implications for marginal basin formation, *J. Geophys. Res.*, submitted.
- [13] P.J. Fox, D.G. Gallo, A tectonic model for ridge-transform-ridge plate boundaries: implications for the structure of oceanic lithosphere, *Tectonophysics* 104 (1984) 205–242.
- [14] K.C. Macdonald, D.A. Castillo, S.P. Miller, P.J. Fox, K.A. Kastens, E. Bonatti, Deep-tow studies of the Vema fracture zone I. Tectonics of a major slow slipping transform fault and its intersection with the Mid-Atlantic Ridge, *J. Geophys. Res.* 91 (1986) 3334–3354.
- [15] D.K. Blackman, D.W. Forsyth, Axial topographic relief associated with ridge-transform intersections, *Earth Planet. Sci. Lett.* 95 (1989) 115–129.
- [16] E. Bonatti, M. Ligi, G. Carrara, L. Gasperini, N. Turko, S. Perfiliev, A. Peyve, P.F. Sciuto, Diffuse impact of the Mid-Atlantic Ridge with the Romanche transform: an ultracold ridge-transform intersection, *J. Geophys. Res.* 101 (1996) 8043–8054.
- [17] D.W. Sparks, E.M. Parmentier, The structure of three-dimensional convection beneath oceanic spreading centers, *Geophys. J. Inter.* 112 (1993) 81–91.
- [18] J. Lin, G.M. Purdy, H. Schouten, J.-C. Sempere, C. Zervas, Evidence from gravity data for focused magmatic accretion along the Mid-Atlantic Ridge, *Nature* 344 (1990) 627–632.
- [19] R.A. Pockalny, P. Gente, W.R. Buck, Oceanic transverse ridges: A flexural response to fracture-zone-normal extension, *Geology* 24 (1996) 71–74.
- [20] E. Bonatti, Vertical tectonism in oceanic Fracture Zones, *Earth Planet. Sci. Lett.* 37 (1978) 369–379.
- [21] D.G. Gallo, P.J. Fox, K.C. MacDonald, A sea beam investigation of the Clipperton Transform Fault: The morphotectonic expression of a fast slipping Transform boundary, *J. Geophys. Res.* 91 (B3) (1986) 3455–3467.
- [22] K.A. Jordahl, M.K. McNutt, H.F. Webb, S.E. Kruse, M.G. Kuykendall, Why there are no earthquakes on the Marquesas fracture zone, *J. Geophys. Res.* 100 (1995) 24431–24447.
- [23] M.C. McCarthy, S.E. Kruse, M.R. Brudzinski, M.E. Rannieri, Changes in plate motions and the shape of Pacific fracture zones, *J. Geophys. Res.* 101 (B6) (1996) 13715–13730.
- [24] S. Allerton, Distortions, rotations and crustal thinning at ridge-transform intersections, *Nature* 340 (1989) 626–632.
- [25] R.C. Searle, GLORIA investigations of oceanic fracture zones; comparative study of the transform fault zone, *J. Geol. Soc. Lond.* 143 (1986) 743–756.
- [26] D. Tamsett, R.C. Searle, Structure and development of the mid-ocean ridge plate boundary in the Gulf of Aden; evidence from GLORIA side scan sonar, *J. Geophys. Res.* 93 (B4) (1988) 3157–3178.
- [27] J.P. Morgan, E.M. Parmentier, Lithospheric stress near a ridge-transform intersection, *Geophys. Res. Lett.* 11 (1984) 113–116.
- [28] R.A. Pockalny, Evidence of transpression along the Clipperton transform: Implications for processes of plate boundary reorganization, *Earth Planet. Sci. Lett.* 146 (1997) 449–464.
- [29] R.A. Livermore, J.S. Tomlinson, R.W. Woollett, Unusual sea-floor fabric near the Bullard fracture zone imaged by GLORIA sidescan sonar, *Nature* 353 (6340) (1991) 158–161.
- [30] L. Sonder, R.A. Pockalny, Anomalously rotated abyssal hills along active transforms: Distributed deformation of oceanic lithosphere, *Geology* 27 (1999) 1003–1006.
- [31] K.A. Kastens, W.B.F. Ryan, P.J. Fox, Structural and volcanic expression of a fast slipping ridge-transform-ridge-plate boundary: sea MARC I and photographic surveys at the Clipperton transform fault, *J. Geophys. Res.* 91 (1986) 3469–3488.
- [32] B.E. Tucholke, J. Lin, M.C. Kleinrock, M.A. Tivey, T.B. Reed, J. Goff, G.E. Jaroslow, Segmentation and crustal structure of the western Mid-Atlantic Ridge flank, 25°25'–27°10'N and 0–29 m.y., *J. Geophys. Res.* 102 (1997) 10203–10223.
- [33] P. Gente, R.A. Pockalny, C. Durand, C. Deplus, M.

- Maia, G. Ceuleneer, C. Mevel, M. Cannat, C. Laverne, Characteristics and evolution of the segmentation of the Mid-Atlantic Ridge between 20°N and 24°N during the last 10 million years, *Earth Planet. Sci. Lett.* 129 (1995) 55–71.
- [34] K. Crane, The spacing of ridge-axis highs: Dependence upon diapiric processes in the underlying asthenosphere?, *Earth Planet. Sci. Lett.* 72 (1985) 405–414.
- [35] B.Y. Kuo, D.W. Forsyth, Gravity anomalies of the ridge-transform system in the South Atlantic between 31° and 34.5°S: Upwelling centers and variations in crustal thickness, *Mar. Geophys. Res.* 10 (1988) 205–232.
- [36] R.S. Detrick, H.D. Needham, V. Renard, Gravity anomalies and crustal thickness variations along the Mid-Atlantic Ridge between 33°N and 40°N, *J. Geophys. Res.* 100 (1995) 3767–3787.
- [37] H. Sloan, P. Patriat, Kinematics of the North American–African plate boundary between 28° and 29°N during the last 10 Ma: Evolution of the axial geometry and spreading rate and direction, *Earth Planet. Sci. Lett.* 113 (1992) 323–341.
- [38] O. Dauteuil, J.P. Brun, Oblique rifting in a slow-spreading ridge, *Nature* 361 (1993) 145–148.
- [39] O. Dauteuil, J.P. Brun, Deformation partitioning in a slow spreading ridge undergoing oblique extension: Mohns Ridge, Norwegian Sea, *Tectonics* 15 (1996) 870–884.
- [40] O. Dauteuil, P. Huchon, F. Quemeneur, T. Souriot, Propagation of an oblique spreading center: the western Gulf of Aden, *Tectonophysics* 332 (2001) 423–442.
- [41] P.R. Shaw, J. Lin, Causes and consequences of variations in faulting style at the Mid-Atlantic Ridge, *J. Geophys. Res.* 98 (1993) 21839–21851.
- [42] S.M. Carbotte, K.C. Macdonald, Comparison of seafloor tectonic fabric at intermediate, fast, and super fast spreading ridges: Influence of spreading rate, plate motions, and ridge segmentation on fault patterns, *J. Geophys. Res.* 99 (1994) 13609–13631.
- [43] C. Rangin, L. Jolivet, M. Pubellier and Thethis Pacific Working Group, A simple model for the tectonic evolution of Southeast Asia and Indonesia regions for the past 43 Ma, *Bull. Soc. Geol. France* 6 (1990) 887–905.
- [44] A. Deschamps, S. Lallemand, J.-Y. Collot, A detailed study of the Gagua Ridge: a fracture zone uplifted during a plate reorganisation in the Mid-Eocene, *Mar. Geophys. Res.* 20 (1998) 403–423.
- [45] I.O. Norton, Tertiary relative plate motions in the North Pacific: The 43 Ma non-event, *Tectonics* 14 (1995) 1080–1094.
- [46] T. Atwater, Plate tectonic history of the Northeast Pacific and western North America, in: E.L. Winterer, Hussong, Donald, Decker, Robert (Eds.), *The Geology of North America*, vol. N, The Eastern Pacific Ocean and Hawaii, Geological Society of America, Denver, CO, 1989, pp. 21–72.
- [47] L. Jolivet, M. Fournier, P. Huchon, V.S. Rozhdestvenskiy, K.F. Sergeev, L.S. Osorbin, Cenozoic intracontinental dextral motion in the Okhotsk-Japan Sea region, *Tectonics* 11 (1992) 968–977.
- [48] K. Okino, S. Kasuga, Y. Ohara, A new scenario of the Parece-Vela Basin genesis, *Mar. Geophys. Res.* 20 (1998) 21–40.